

A new apparent quasar pair: Q2225-403A,B

R. Decarli^{1*}, A. Treves¹, R. Falomo²

¹ *Università degli Studi dell'Insubria, via Valleggio 11, 22100 Como, Italy*

² *INAF - Osservatorio Astronomico di Padova, Vicolo dell'Osservatorio 5, 35122, Padova, Italy*

ABSTRACT

We report the serendipitous discovery of a previously unknown quasar at $10.5''$ from Q2225-403 ($z = 2.410$). The observation of the broad emission line of $\text{Mg II}_{\lambda 2798}$ and of the surrounding Fe II multiplets indicates that the companion quasar is at $z = 0.932$. The spectrum of Q2225-403 shows a number of absorption lines, the most noteworthy is the Mg II line at the same redshift of the companion, suggesting that we are probing the gas within the halo ~ 80 kpc from the closer quasar. From high resolution NIR images we were able to resolve the host galaxies of the two quasars. Basing on the known surface density of quasars in the 2dF survey we estimate that the probability of finding such a close pair is $\lesssim 1$ per cent.

Key words: galaxies: active - quasars: general - quasars: individual: Q2225-403

1 INTRODUCTION

Quasar pairs can be classified in physical pairs, gravitational lenses and projected associations. Quasars in physical pairs are gravitationally interacting or belong to the same structure (e.g., a cluster of galaxies). They represent a formidable tool to improve our understanding of the evolution of galaxy and dark matter clustering with Cosmic Time, since they can be traced up to very high redshift (Komberg Kravtsov & Lukash 1996; Shen et al. 2008). They can also provide information about the role of galaxy interactions in triggering nuclear activity (e.g., Kang & Im 2007; Foreman Volonteri & Dotti 2008). Gravitationally lensed quasars allow an unparalleled insight of the lens distribution of matter (e.g. Wittman et al. 2000; Chierigato Miranda & Jetzer 2007). Projected pairs can be used as probes of the spatial structure and ionization properties of intervening intergalactic medium (e.g. Jakobsen et al. 1986; D’Odorico et al. 2008; Gallerani et al. 2008) and, through the transverse proximity effect (Schirber, Miralda-Escudé & McDonald 2004), of the megayear variability and duty cycle of quasars.

Up to now, only a dozen of apparent quasar pairs with angular separation less than 10 arcsec are known. Recent large field surveys, such as the Sloan Digital Sky Survey (Adelman-McCarthy et al. 2008), collected spectra of $\sim 100,000$ quasars, and probed their large scale (> 0.5 Mpc) clustering. Nevertheless, the limit due to the finite physical dimension of the spectroscopic fibers prevented the obser-

vation of objects with angular separations less than $55''$, making this survey unsuitable for finding quasar pairs.

In the framework of the study of the $M_{\text{BH}}-L_{\text{host}}$ relation throughout Cosmic Time (Decarli et al., 2009b in preparation), we collected high-resolution NIR imaging (Kotilainen et al. 2009, K09) and optical spectroscopy (Decarli et al., 2009a, in preparation) of Q2225-403 (hereafter, quasar A), a $z = 2.410$ quasar first reported by Hewitt & Burbidge (1993). We set the slit orientation so that we simultaneously observed both quasar A and the $10.5''$ North-East source with similar magnitude (see figure 1). The spectrum of the companion shows it is a quasar at $z = 0.932$ (quasar B). In this paper we discuss the properties of this system together with a statistical analysis of apparent quasar pairs.

Throughout the paper, we adopt a concordance cosmology with $H_0 = 70$ km/s/Mpc, $\Omega_m = 0.3$, $\Omega_\Lambda = 0.7$.

2 OBSERVATIONS AND DATA REDUCTION

2.1 Spectroscopic data

Spectroscopy was collected at the European Southern Observatory (ESO) 3.6m telescope in La Silla (Chile; program ID: 079.B-0304(A)) on September, 9th, 2007: see Decarli et al. 2009a for details. Spectra were obtained through a $1.2''$ slit in the wavelength 4100–7500 Å with a spectral resolution $R \sim 400$. Standard recipes for data reduction were adopted. Three individual exposures, for a total of 71 min integration time, were acquired. We set the Position Angle to 131.6° , in order to observe simultaneously both Q2225-403 A and B. Two-dimensional spectra were

* E-mail: roberto.decarli@mib.infn.it

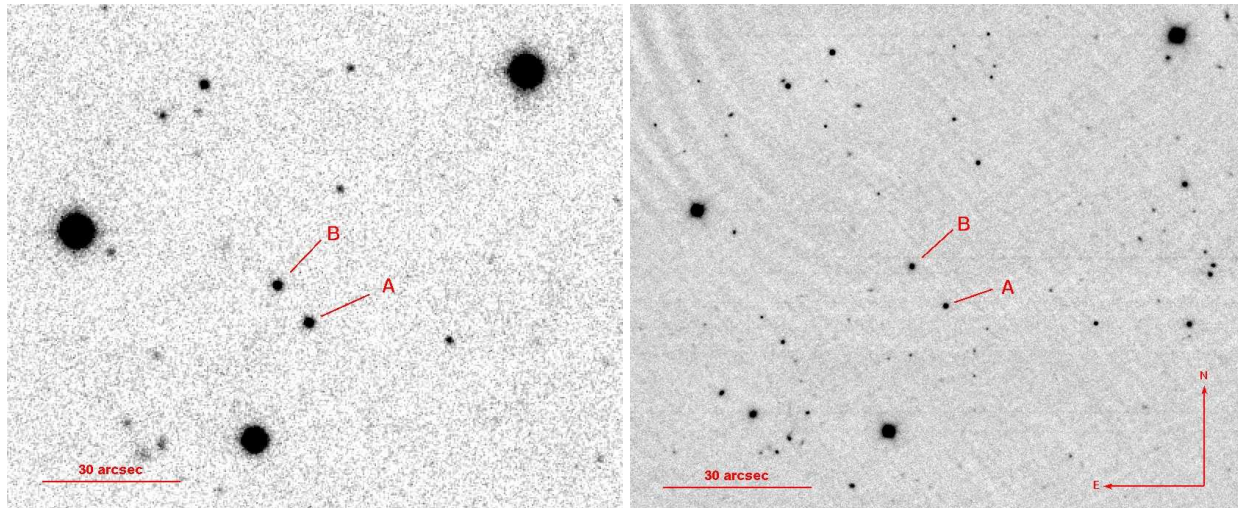


Figure 1. The field of quasar pair Q2225-403A,B in R (*left*), observed at the ESO/3.6m telescope and in Ks (*right*) taken at the ESO/VLT. ‘A’ marks the original quasar at $z = 2.410$, ‘B’ refers to the new $z = 0.932$ quasar.

bias subtracted, flat fielded, re-aligned and combined scaling according to signal to noise. One-dimensional spectra were extracted and wavelength- and flux-calibrated. The same calibration procedures were adopted for the two spectra. Absolute flux calibration was performed using corollary R-band photometry (see figure 1, *left*). Final spectra were then de-reddened according to the E(B-V) maps from Schlegel Finkbeiner & Davis (1998).

2.2 Imaging data

A deep Ks-band image of Q2225-403 field was obtained using ISAAC (Moorwood et al. 1998), mounted on UT1 (Antu) of ESO/VLT (see figure 1, *right*). Q2225-403 was part of a sample of 16 objects, selected from the VCV06 catalogue in order to have relatively faint nuclear absolute magnitudes ($-26 > M_V > -27$), $2 < z < 3$ and 2–3 bright stars in the close field in order to accurately characterize the PSF (this is mandatory for the study of the host galaxies of bright quasars). We refer to K09 for details on the observations and data reduction. The average seeing was 0.46 ± 0.05 arcsec and the sky brightness was 13.34 mag/arcsec². Photometric calibration was performed through the comparison with 2MASS magnitudes of bright stars available in the field. The estimated photometric accuracy is 0.05 mag.

3 RESULTS

Quasar B (RA_{J2000}=22:28:50.4; Dec_{J2000}=-40:08:27) is not present in the catalogue by Veron-Cetty & Veron (2006, hereafter VCV06), nor in the NED or Simbad archives. It appears in the USNO-B1.0 catalogue (source ID: 0498-0814048, $m_R = 20.0$, $m_B = 20.4$, grossly consistent with the photometry of our R-band image, $m = 19.6$). The optical spectrum clearly shows the broad Mg II line surrounded by Fe II multiplets (see Figure 2), leaving no doubt on the source nature. The peak of the Mg II line is observed at 5406 Å, yielding $z = 0.932$.

A number of absorption systems are apparent in the

Table 1. List of the main observed absorption features. Atmospheric and Galactic lines are dropped. (1) Peak wavelength. (2) Measured Equivalent Width. (3) Identification. Uncertain classifications are marked with ‘?’ . (4) Rest frame Equivalent Width, assuming the redshift in column (3). (5) Spectrum where the lines are detected.

λ Å	EW Å	Identification	EW _r Å	Object
(1)	(2)	(3)	(4)	(5)
4547	3.8 ± 1.4	MgII $z = 0.625?$	2.3 ± 0.9	A
5408	2.3 ± 0.7	MgII $z = 0.932?$	1.2 ± 0.4	A
4661	2.3 ± 0.6	MgII $z = 0.665?$	1.4 ± 0.4	B
5833	4.4 ± 1.0	FeI ₃₀₂₀ $z = 0.932?$	2.3 ± 0.5	B
7393	7.3 ± 3.3	FeI ₃₈₃₀ $z = 0.932$	3.8 ± 1.7	B

spectra of Q2225-403A,B (see Table 1). In quasar B, an absorption at 7393 Å is detected, that is consistent with the FeI₃₈₃₀, typical of early-type galaxies, at $z = 0.932$. Other absorption lines are detected in the spectrum of quasar A at 4547 Å and B at 4661 Å. Assuming that they are also produced by Mg II_{λ2800}, they correspond to $z = 0.625$ and $z = 0.665$ respectively. Since each feature is observed only in one spectrum, we argue that the amount of intervening gas of the two clouds drop in a relatively small spatial scale ($\lesssim 75$ kpc). Furthermore, in the spectrum of quasar A a faint feature is present at 5408 Å. (see Figure 2) This absorption is clearly present in each of the 3 individual exposures of the spectrum. Therefore we are confident that it is a real feature. The most likely identification of this line is with the Mg II doublet ($\lambda\lambda = 2796, 2804$ Å), at the same redshift of quasar B, $z = 0.932$. At the resolution of our observations, the two components of the doublet are blended. The presence of this absorption reveals an extended halo around the host galaxy of quasar B at the projected distance of 83 kpc.

From the analysis of NIR imaging data, we are able to detect the host galaxy of both quasars. For quasar B, the Ks-band roughly corresponds to the rest-frame J. We

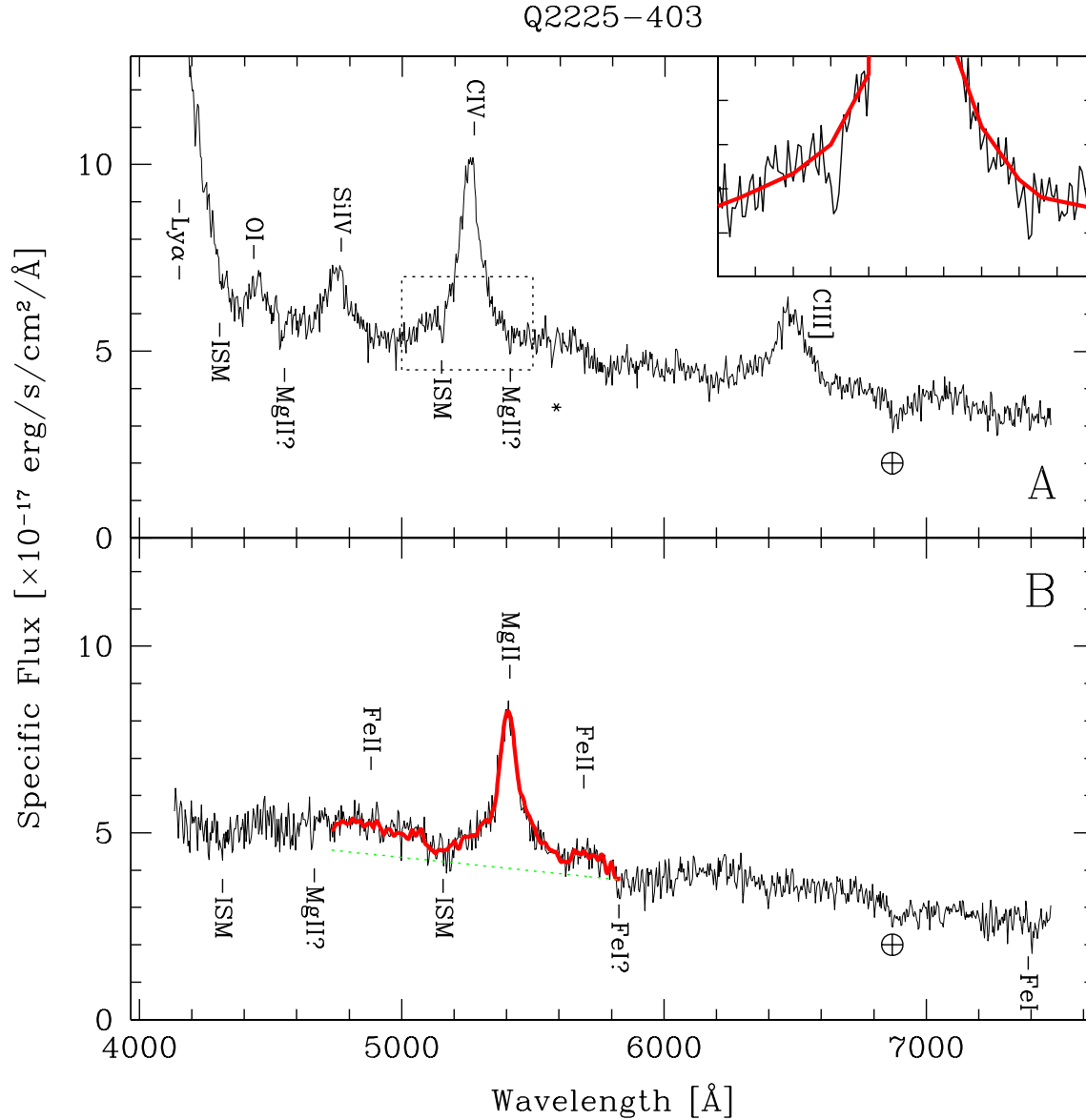


Figure 2. Spectra of quasars Q2225-403 A and B. Main emission and absorption lines are labelled (see also table 1). The \oplus symbols mark main atmospheric absorptions. The asterisk refers to the residual of the strong night sky line at 5577 Å. ISM labels the features due to the Galactic interstellar medium. *Top panel* – The inset in the upper panel highlights the 5000–5500 Å region, with the absorption feature of Mg II at the bottom of the broad C IV emission line. The bold line represent the fit of the C IV emission profile. The inset is also marked in the spectrum of quasar A with a dotted box. *Bottom panel* – The thick (red) line is the model of the Mg II+Fe II emission (Vestergaard & Wilkes 2001) in the wavelength range 4700–5800 Å, supporting the line identification and, hence, our estimate of quasar B redshift. The dotted (green) line shows the underlying continuum.

convert the observed magnitude into R-band by assuming the elliptical galaxy template by Mannucci et al. (2001), yielding $M_R(\text{host}) = -23.2$. The galaxy is well resolved and modelled with a de Vaucouleurs profile with scale radius $R_{\text{eff}} = 5.2$ kpc (see Figure 3). The nuclear component has $M_R(\text{nuc}) = -22.5$. Assuming the quasar template in Francis et al. (1991), we infer $R-i = -0.04$. The derived i -band nuclear magnitude places source B at the faint end of quasar luminosity function, but matching the usual $M_i < -22$ criterion for quasar classification (e.g. Richards et al. 2006).

In a study of quasar–galaxy projected associations, Kacprzak et al. (2007) found a correlation between the EW of $\text{Mg II}_{\lambda 2796}$ and the asymmetry of the galaxy, suggesting a connection between the intervening metal absorption systems and the properties of the galaxy environment. According to this relationship, the stronger are the absorptions, the more disturbed is the morphology of the galaxy. In our case, we are unable to resolve the $\text{Mg II}_{\lambda 2796}$ line. If we assume a ratio between the two components of the Mg II doublet of 1.7, we infer $\text{Mg II}_{\lambda 2796} = 0.8$. We note that a weak indication of asymmetry is apparent in the faintest surface bright-

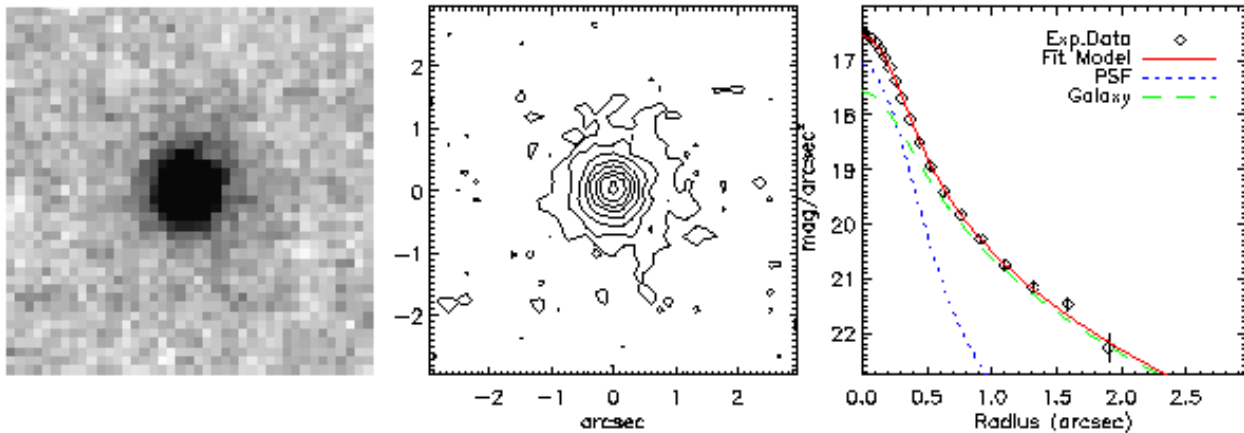


Figure 3. Analysis of the image of Q2225-403B. *Left* – the observed Ks-band image of the quasar; *Centre* – same image in isophotal contours; *Right* – the best-fit light profile model. See also http://www.dfm.uninsubria.it/astro/qso_host/.

ness level of the host galaxy of quasar B, that is in qualitative agreement with the trend suggested by Kacprzak et al. (2007).

4 AN INVENTORY OF APPARENT QUASAR PAIRS

Due to the importance of quasar pairs of the type discussed here, we made an inventory of similar systems starting from the VCV06 catalogue. Out of ~ 85000 quasars, we found 19 pairs with angular separation $\theta < 10''$ and line-of-sight velocity differences exceeding 3000 km/s (hence excluding physical pairs). They are listed in Table 2. We note that only 11 systems out of 19 have been already considered in the framework of quasar pairs. On average, apparent pairs reported in Table 2 have $\langle z(\text{near}) \rangle \approx 1.4$ and $\langle \Delta z \rangle \approx 0.5$. Our case represents a record in terms of redshift difference. Other three systems are reported with the nearer quasar at $z < 1$, where a detailed study of the host galaxy luminosity and morphology is feasible. The typical projected distances at $z(\text{near})$ are ~ 60 kpc.

A number of apparent quasar pairs have been proposed as anomalous associations (e.g. Burbidge Hoyle & Schneider 1997; Galianni et al. 2005) with respect to chance alignments. We estimate that the number of systems reported in Table 2 is consistent with the assumption of chance superposition. In fact, the probability that, given a quasar, a projected companion can be found within a given angular separation θ follows the Poisson statistics: $P(< \theta) \approx \lambda$. Here λ is the expected number of quasars in the solid angle defined by θ , $\lambda = \rho(< m) \pi \theta^2$, and $\rho(< m)$ is the number density of quasars brighter than a given magnitude m . We refer to the 2dF survey (Croom et al. 2004): $\rho(m_b < 20) = 13.8$ quasars per square degree, in good agreement with the values from the SDSS (see Yanny et al. 2000). Hence the probability of finding a quasar with $m_b \lesssim 20$ within a $10.5''$ circle is $\sim 4 \times 10^{-4}$.

5 CONCLUSIONS

We report the discovery of an apparent quasar pair with angular separation of $10.5''$. Q2225-403A,B is the only apparent pair of quasars for which both the host galaxies have been resolved. Their Ks-band apparent magnitudes ($m_A(\text{host}) = 18.51$; $m_B(\text{host}) = 17.44$) are consistent with those expected for typical quasar host galaxies at the distance indicated by their redshift. The discovery of an intervening absorption system in quasar A at the same redshift of B reveals an extended halo around the nearest object.

Based on the known surface density distribution of quasars we find that the *a priori* probability of finding such a pair in our survey is of the order of 0.6 per cent and the discovery of the absorption system on the spectrum of quasar A at the same z of quasar B is a clear evidence that these two objects are an apparent pair.

We propose a list of apparent quasar pairs which deserve a specific study to investigate the properties of the extended halo around quasar host galaxies.

ACKNOWLEDGMENTS

We thank Marzia Labita for useful discussions. This work was based on observations made with the ESO/3.6m telescope in La Silla and with the ESO/VLT in Paranal. This research has made use of the *VizieR Service*, available at <http://vizier.u-strasbg.fr/viz-bin/VizieR> and of the NASA/IPAC Extragalactic Database (NED) which is operated by the Jet Propulsion Laboratory, California Institute of Technology, under contract with the National Aeronautics and Space Administration.

REFERENCES

- Adelman-McCarthy J.K., et al., 2008, ApJS, 175, 297
- Burbidge G., Hoyle F., Schneider P., 1997, A&A, 320, 8
- Chierigato M., Miranda M., Jetzer P., 2007, A&A, 474, 777

Table 2. Quasar apparent pairs with $\theta < 10''$ from the VCV06 catalogue, in a comparison with Q2225-403A,B. (1–4) z , RA, Dec and m_V of the quasar with the lower z . (5–8) the same for the higher z quasar. (9) angular separation. (10) projected separation assuming the redshift of the lower- z quasar. (11) redshift difference. (12) references (only those references concerning quasar pairs are included): *a* - Burbidge Hoyle & Schneider (1997); *b* - Sluse et al. (2003); *c* - Hennawi et al. (2006); *d* - Myers et al. (2007).

Nearer quasar				Farther quasar				θ	Proj.sep.	Δz	Ref
z	RA(J2000)	Dec(J2000)	m_V	z	RA(J2000)	Dec(J2000)	m_V	["]	[kpc]	(11)	(12)
(1)	(2)	(3)	(4)	(5)	(6)	(7)	(8)	(9)	(10)	(11)	(12)
<i>Known quasar pairs</i>											
1.545	00:02:12.6	-00:53:11	20.46	2.206	00:02:12.1	-00:53:09	19.58	6.3	53	0.661	<i>c</i>
2.030	00:40:18.2	+00:55:31	18.72	2.086	00:40:18.7	+00:55:26	19.67	7.7	64	0.056	<i>c</i>
1.296	01:22:12.7	+14:10:54	19.91	1.579	01:22:13.1	+14:10:52	20.03	8.1	67	0.283	<i>c</i>
1.442	02:41:06.9	+00:10:27	19.89	1.673	02:41:07.4	+00:10:28	20.87	9.8	82	0.231	<i>c</i>
2.180	08:14:20.4	+32:50:16	19.86	2.210	08:14:19.6	+32:50:19	20.33	9.5	78	0.030	<i>c</i>
1.340	09:02:35.7	+56:37:56	20.30	1.390	09:02:35.4	+56:37:51	20.63	6.6	55	0.050	<i>c, d</i>
1.627	10:12:15.8	-03:07:08	18.90	2.746	10:12:15.8	-03:07:03	17.60	4.5	38	1.119	<i>a, b</i>
1.142	12:04:50.5	+44:28:35	19.20	1.814	12:04:50.7	+44:28:33	19.42	3.8	31	0.672	<i>c, d</i>
2.379	12:25:45.7	+56:44:40	19.36	2.390	12:25:45.2	+56:44:45	20.51	7.4	60	0.011	<i>c</i>
2.001	12:49:48.1	+06:07:08	20.42	2.376	12:49:48.2	+06:07:13	20.37	3.9	32	0.375	<i>c, d</i>
0.436	15:50:43.7	+11:20:47	17.23	1.901	15:50:44.0	+11:20:47	18.78	4.4	24	1.465	<i>a, b</i>
<i>New quasar pairs</i>											
1.310	00:39:54.3	-27:25:23	20.61	2.100	00:39:54.1	-27:25:14	20.64	9.9	83	0.790	
1.264	00:39:54.8	-27:25:20	20.26	1.310	00:39:54.3	-27:25:23	20.61	4.3	35	0.046	
1.333	01:10:50.8	-27:19:51	20.10	2.261	01:10:51.4	-27:19:57	20.84	9.3	78	0.928	
1.586	03:42:12.4	-44:16:41	19.20	2.077	03:42:12.6	-44:16:36	19.70	5.7	48	0.491	
1.519	10:16:36.3	-02:34:22	19.55	2.617	10:16:36.4	-02:34:12	20.31	8.9	75	1.098	
0.649	10:51:26.8	-02:27:20	19.43	1.160	10:51:26.3	-02:27:17	19.53	8.0	55	0.511	
0.888	11:18:47.9	+40:26:43	20.70	1.129	11:18:48.6	+40:26:47	19.05	7.9	61	0.241	
1.863	23:33:05.3	-28:00:54	20.33	1.970	23:33:04.7	-28:00:55	19.72	7.5	63	0.107	
<i>This paper</i>											
0.932	22:28:50.4	-40:08:27	20.20	2.410	22:28:49.9	-40:08:34	20.10	10.5	83	1.478	

Croom S.M., Schade D., Boyle B.J., Shanks T., Miller L., Smith R.J., 2004, ApJ, 606, 126
D'Odorico V., et al., 2008, MNRAS, 389, 1727
Foreman G., Volonteri M., Dotti M., 2008, ApJ submitted
Francis P.J., Hewett P.C., Foltz C.B., Chaffee F.H., Weymann R.J., Morris S.L., 1991, ApJ, 373, 465
Galianni P., Burbidge E.M., Arp H., Junkkarinen V., Burbidge G., Zibetti S., 2005, ApJ, 620, 88
Gallerani S., Ferrara A., Fan X., Choudhury T.R., 2008, MNRAS, 386, 359
Hennawi J.F., Strauss M.A., Oguri M., Inada N., Richards G.T., Pindor B., Schneider D., Becker R.H., et al., 2006, AJ, 131, 1
Hewitt A. & Burbidge G., 1993, ApJ Suppl., 87, 451
Jakobsen P., et al., 1986, ApJ Letters, 303, 27
Kacprzak G.G., Churchill C.W., Steidel C.C., Murphy M.T., Evans J.L., 2007, ApJ, 662, 909
Kang E., Im M., 2007, AAS, 211, 9609
Komborg B.V., Kravtsov A.V., Lukash V.N., 1996, MNRAS, 282, 713
Kotilainen J.K., Falomo R., Decarli R., Treves A., Uslenghi M., Scarpa R., 2009, ApJ submitted
Mannucci F., Basile F., Poggianti B.M., Cimatti A., Daddi E., Pozzetti L., Vanzì L., 2001, MNRAS, 326, 745
Moorwood A., Cuby J.-G., Biereichel P., Brynnel J., Delabre B., Devillard N., van Dijksseldonk A., Finger G., et al., 1998, ESO Messenger, 94, 7
Myers A.D., Brunner R.J., Richards G.T., Nichol R.C., Schneider D.P., Bahcall N.A., 2007, ApJ, 658, 99

Richards G.T., Strauss M.A., Fan X., Hall P.B., Jester S., Schneider D.P., Vanden Berk D.E., Stoughton C., et al., 2006, AJ, 131, 2766
Schirber M., Miralda-Escudé J., McDonald P., 2004, ApJ, 610, 105
Schlegel D.J., Finkbeiner D.P., Davis M., 1998, ApJ, 500, 525
Shen Y., Strauss M.A., Ross N.P., Hall P.B., Lin Y.T., Richards G.T., Schneider D.P., Weinberg D.H., et al., 2008, arXiv:0810.4144
Sluse D., Surdej J., Claeskens J.-F., De Rop Y., Lee D.W., Iovino A., Hawkins M.R.S., 2003, A&A, 397, 539
Veron-Cetty M.P., & Veron P., 2006, A&A, 455, 773
Vestergaard M., Wilkes B.J., 2001, ApJ Suppl., 134, 1
Wittman D.M., et al., 2000, Nature, 405, 143
Yanny B., Newberg H.J., Kent S., Laurent-Muehleisen S.A., Pier J.R., Richards G.T., Stoughton C., Anderson J.E., et al., 2000, ApJ, 540, 825

This paper has been typeset from a \LaTeX file prepared by the author.